

## CHEMICALLY SELECTIVE LASER ION-SOURCE FOR THE CERN-ISOLDE ON-LINE MASS SEPARATOR FACILITY

V.I. Mishin<sup>1)</sup>, V.N. Fedoseyev<sup>1)</sup>, H.-J. Kluge<sup>2)</sup>, V.S. Letokhov<sup>1)</sup>, H.L. Ravn<sup>3)</sup>,  
F. Scheerer<sup>2)</sup>, Y. Shirakabe<sup>4)</sup>, S. Sundell<sup>3)</sup>, O. Tengblad<sup>3)</sup>

and the ISOLDE Collaboration, PPE Div., CERN, Geneva, Switzerland

### ABSTRACT

Radioactive atoms produced in proton-induced nuclear reactions and released from thick targets have been ionized resonantly by laser radiation in a hot tube connected to the target container. Pulsed tuneable lasers with a repetition rate as high as 10 kHz have been applied for stepwise resonant excitation and photoionization in the last step. In this way the efficiency and selectivity of the target and ion source system which serves as injector to the on-line isotope separators at CERN-ISOLDE could be improved. In a series of off-line and on-line studies the ionization of Sn ( $E_i = 7.3\text{eV}$ ), Tm ( $E_i = 6.2\text{eV}$ ), Yb ( $E_i = 6.2\text{eV}$ ) and Li ( $E_i = 5.4\text{eV}$ ) was investigated. An ionization efficiency of up to 15% was obtained for Yb. The ratio of the laser-ionized and surface-ionized ion currents was measured as function of temperature for different ionization-cavity materials (W, Ta, Nb and TaC). It was shown that this ratio, (i.e. the selectivity) rises for Tm from 10 to 10000 with falling temperature and is strongly depending on the material. Since the lasers are pulsed the ion beam becomes bunched with a pulse width of about 10-50  $\mu\text{s}$ . This width is strongly dependent on the potential drop along the tube (caused by the electric current used for heating the tube) and on the alignment of the laser beams with respect to the tube axis. The selectivity could be further improved by a factor of 10 using a gated detection of the bunched ion beam.

(IS01)

(To be submitted to: Nuclear Instruments and Methods in Physics Research B)

---

1) Institute of Spectroscopy, 142092 Troitzk, Russia

2) Institut für Physik, Johannes-Gutenberg Universität, D-6500 Mainz, Fed. Rep. Germany

3) CERN, CH-1211 Geneva 23, Switzerland

4) Institute of Nuclear Studies, University of Tokyo, Tanashi, 188 Tokyo, Japan

## 1. INTRODUCTION

One of the main problems of ion sources used at on-line mass separators for radioactive beam production is to obtain chemically pure ions-beams of the various elements. At present, the ion sources which are most widely used for this purpose are based on surface ionization or ionization in a gas-discharge plasma [1]. However, as a result of the thermal character of these processes the ionization is in many cases non-selective with respect to the different chemical elements. Hence, the separated ion beams are contaminated by isobars, which significantly complicates, and in a number of cases renders impossible, the study of the nuclear properties of radioactive isotopes.

The process of resonance laser ionization of atoms is of non-thermal nature [2]. The atom is ionized whenever the laser radiation frequencies coincide with the atomic transition frequencies. Since the atom of each element has its own specific energy level structure the ionization process has an exceptionally high chemical selectivity. It should be remarked that the efficiency of photo-ionization is also high so that the ion yield may reach tens of percent. This is also true for elements with a high ionization potential.

In view of its high efficiency and selectivity, the method of laser ionization of atoms is widely used in different branches of physics and in particular for studying the properties of radioactive nuclei [3 ,4]. However, when it is used as an ion source for a mass separator, it is necessary to substantially increase the overall ionization efficiency. For this purpose the method of resonance laser ionization of atoms in a hot cavity was developed [5,6]. In order further to study this concept a series of off-line and on-line tests were performed with the mass separators of the CERN-ISOLDE collaboration [7]. A schematic layout of the experiment is shown in Fig. 1.

Chapter 2 describes in detail the operating principle of such sources. The properties of the capillary version of the source is discussed in chapter 3 followed in chapter 4 by the details of the lasers used and the target and ion source mechanical design. Studies of the selectivity and efficiency as function of capillary tube material are described in chapter 5. Results on optimization of the source efficiency and selectivity for rare earth elements and tin are given in chapter 6 together with an investigation of the ionization of Li. The pulse structure of the ion beam is discussed in chapter 7. Finally chapter 8 contains the conclusions and outlines the further improvements and use of the source.

## 2. OPERATING PRINCIPLE OF THE LASER ION-SOURCE

Resonance laser ionization of atoms operates as shown in Fig. 2. Laser radiation at frequencies  $\omega_1$  and  $\omega_2$  excites the atom resonantly via atomic intermediate states, and radiation at frequency  $\omega_3$  ionizes it. The ionization of an excited atom can be done non resonantly through

the continuum or resonantly through an autoionizing or Rydberg state. Radiation energy equal to a few mJ/cm<sup>2</sup> is sufficient in order to saturate the resonance transitions. At this value, a significant fraction of the atoms interacting with the laser light will be ionized. Such an energy density can be obtained from dye lasers pumped by copper vapour lasers (CVL). They provide a high pulse repetition rate and, consequently, a high chance for interaction of the atoms with the laser light which results in an efficient ionization. In case of ionization through the continuum the pulse energy of dye lasers is insufficient for saturation of a transition, however, CVL radiation can be used directly for ionization of excited atoms.

Most simply, the ionization of elements of low volatility is performed in an atomic beam (Fig. 3a). The atomic beam interacts with a laser beam which intersects it over a certain distance. The efficiency of ionization in this case can be estimated according to the formula

$$\eta_{\text{atomic beam}} = \left(\frac{\alpha^2}{2\pi}\right) \times \left(\frac{L \times f}{v}\right) \times \eta_{\text{photoion}} \quad (1)$$

where  $\alpha$  is the angular divergence of the atomic beam,  $L$  is the diameter of the laser beam in the direction of motion of the atoms,  $v$  is the thermal velocity of the atoms,  $f$  is the repetition rate of the laser pulses, and  $\eta_{\text{photoion}}$  is the laser-ionization efficiency per pulse. The first term in this formula relates to losses in forming the atomic beam (spatial overlap), and usually amounts to 1-3%. The value of the second term is defined by the temporal overlap of the continuous atomic beam and the pulsed lasers. It is negatively affected by a low repetition rate of the laser pulses and a short interaction time of the atoms with the radiation. If the pulse repetition rate is high, for example  $f = 10^4 \text{ s}^{-1}$ , and the laser beam has a diameter of  $L = 5 \text{ mm}$ , then this term is roughly 10%. The efficiency  $\eta_{\text{photoion}}$  depends on the energy of the laser pulse, the population of the ground state and the cross-sectional area of the laser beam. For an average radiation power of dye lasers of  $P \approx 1 \text{ W}$ , and a cross-sectional area of the laser beam equal to  $\approx 5 \text{ mm}^2$ ,  $\eta_{\text{photoion}} \approx 20\%$ . A reduction in the diameter of the laser beam leads on the one hand to an increase in the energy density of the laser radiation and hence to an increase in  $\eta_{\text{photoion}}$ ; on the other hand the fraction of atoms which interacts with the laser radiation is reduced. In this case, the overall ionization efficiency  $\eta_{\text{atomic beam}}$  is practically unchanged. In experiments with atomic beams it is usually possible to achieve an overall ionization efficiency of the atoms fed into the atomizer of  $\eta_{\text{atomic beam}} \approx 0.05\%$ .

It is possible to substantially increase this value if conditions are provided whereby almost all the atoms interact with the laser radiation. This particular geometry for performing the experiment was suggested by the authors of ref. [5] and [6]. Atoms of the element under investigation, located in a closed hot cavity, are irradiated with laser beams fed into the cavity via a small aperture which is also used for extraction of the photoions (Fig. 3b).

If the repetition frequency for the laser pulses is high enough it is easy to provide conditions where the probability for ionizing of the atom, before it leaves the cavity via the aperture through which the laser radiation is introduced, becomes close to unity. The ionization efficiency of the atoms in the cavity can be calculated from eq. 2 of ref. [8]

$$\eta_{\text{cavity}} = \frac{f \times \eta_{\text{photoion}}}{\left( f \times \eta_{\text{photoion}} + \frac{v}{4L} \right)} \quad (2)$$

where  $L$  now becomes the length of the cavity. It takes into account the reduction in concentration of atoms in the cavity as a result of photo-ionization and extraction. In this case of saturation ( $\eta_{\text{photoion}} = 1$ ) the efficiency is independent of the diameter  $d$  of the aperture. In contrast to the ionization in an atomic beam, the ionization efficiency can in case of non saturation be increased by a sharper focusing of the laser beams and a smaller aperture. For  $d = 1$  mm it can reach  $\eta_{\text{photoion}} \approx 80\%$ . As a result, the overall efficiency of atom ionization in a hot cavity can for typical parameters of  $L = 1$  cm and a pulse repetition rate of  $f = 10^4$  s<sup>-1</sup> attain a value of  $\eta_{\text{cavity}} \approx 25\%$ . By means of this method of laser ionization, a number of experiments were carried out on the ultra-sensitive detection of different elements [8,9,10].

It is possible to increase further  $\eta_{\text{cavity}}$  of the source by making it in the form of a thin capillary tube, having a length  $L$  but a diameter  $d \ll L$  equal to the diameter of the laser beam (Fig. 3c). The rate of atomic effusion out of such a capillary is reduced by approximately the factor  $L/d$  as compared to a cavity having a typical dimension of  $L$  and given by

$$\eta_{\text{capillary}} = \frac{f \times \eta_{\text{photoion}}}{\left( f \times \eta_{\text{photoion}} + \frac{d \times v}{4L^2} \right)} \quad (3)$$

The ionization efficiency of atoms entering the capillary will thus be enhanced compared to the ionization efficiency of atoms in the cavity with  $L \approx d$ .

Some practical problems arises in connection with the use of the hot capillary. Depending on the cavity material and its temperature the element to be ionized may be adsorbed on the tube material resulting in losses or delays affecting short-lived species. Therefore, the wall temperature of the cavity should be kept sufficiently high, more than 2000 K. For mechanical stability and a long service life the only useful tube materials are refractory metals like Ta, W, Nb or chemical compounds like carbides and oxides. In addition nonselective surface ionization may affect the selectivity of such a laser ion-source.

However, as described in detail in the next chapter, the effective extraction of photo-ions from the hot metal capillary is assisted by an ion storage effect. As a result of strong electron emission inside the capillary a negatively charged well is formed which prevents the positive

ions created inside it from striking the wall [11]. This allows the potential applied across the tube for heating to eject the ions formed.

### 3. IONIZATION IN A HOT CAVITY

The phenomena occurring in a hot cavity have been examined in detail in a number of publications [12,13]. We shall mention only the main equations. In the plasma inside the cavity, when a thermodynamic equilibrium is established, the concentrations of ions  $n_i^{\text{volume}}$ , electrons  $n_e^{\text{volume}}$  and atoms  $n_0$  are given by the Eggert-Saha equation

$$\frac{n_e^{\text{volume}} \times n_i^{\text{volume}}}{n_0} = \left(\frac{2g_i}{g_0}\right) \times \left(\frac{2\pi \times m \times k \times T}{h^2}\right)^{\frac{3}{2}} \times \exp\left(\frac{-W_i}{k \times T}\right) \quad (4)$$

where  $g_i$  and  $g_0$  represent the statistical weights of the ion and atom respectively,  $W_i$  is the ionization potential of the atom, and  $T$  is the absolute wall temperature. The electron density at the walls is described by the Richardson equation

$$n_e^{\text{surface}} = 2 \left(\frac{2\pi \times m \times K \times T}{h^2}\right)^{\frac{3}{2}} \times \exp\left(\frac{-\Phi}{k \times T}\right) \quad (5)$$

where  $\Phi$  is the work function of the wall material. From (4) which is also valid at the surface of the walls and (5) it is possible to find the degree of ionization of the atoms at the walls

$$\alpha = \frac{n_i^{\text{surface}}}{n_0} = \left(\frac{g_i}{g_0}\right) \times \exp\left[\frac{(\Phi - W_i)}{k \times T}\right] \quad (6)$$

The surface ionization efficiency of the cavity is given by

$$\epsilon_{\text{surface}} = \frac{n_i^{\text{volume}}}{n_i^{\text{volume}} + n_0} \quad (7)$$

Assuming that inside the cavity the plasma is in thermodynamic equilibrium and quasi-neutral ( $n_i^{\text{volume}} = n_e^{\text{volume}}$ ), the following equation can be obtained for the degree of ionization in the volume [12]:

$$\frac{n_i^{\text{volume}}}{n_0} = C^* \times \exp\left(\frac{-W_i}{k \times T}\right) \quad (8)$$

where  $C^*$  is a parameter only dependent on  $T$  and the plasma density  $n_e$ . The plasma has, in relation to the walls, a negative potential  $\Phi_p$  such that

$$\frac{n_i^{\text{volume}}}{n_i^{\text{surface}}} = \frac{n_e^{\text{surface}}}{n_e^{\text{volume}}} = \exp\left(\frac{-e \times \Phi_p}{k \times T}\right) \quad (9)$$

From (8) it can be seen that, in the case of thermodynamic equilibrium, the degree of ionization does not depend on the work function of the wall material  $\Phi$ , but is determined only by the ionization potential of the atom. The value of the plasma potential amounts to several volts at temperatures above 2000 K. This means that ions inside the plasma cannot become neutralized at the walls since the energy of their thermal motion is insufficient to overcome the potential barrier.

Figure 4 illustrates schematically the movement of an ion in the capillary after its formation by laser radiation.

#### 4. DESIGN OF THE LASER ION-SOURCE

The laser ion-source (Fig. 5) was designed on the basis of the standard ISOLDE thick target system, [1]. The ionizer was the only part to be subjected to changes which were minimal. The laser beams were fed into the mass separator from the magnet side via a quartz window fitted in the vacuum chamber and reached the ionizer tube through the extraction electrode (Fig. 1). The ionizer tube was made of tantalum with an inside diameter of  $d = 1$  mm, an outside diameter of 2 mm and a length of  $L = 3$  cm. The voltage applied to the tube (for heating and ion extraction) corresponded to an electrical field of  $E = 0.5$  V/cm which resulted in a current of typically 150 A and a temperature of  $T = 2000$  K. The laser beams were focused to a diameter of approximately 1 mm. The light spot at the entrance of the capillary and the central part of the capillary itself were observed by means of a theodolite (Fig. 1). The theodolite made it also possible to precisely adjust the laser beam to the axis of the capillary during the experiment without entering the radioactive area where the target was located.

The laser system consisted of three dye lasers, pumped by the radiation of two copper vapour lasers, one operating as oscillator, the other one as amplifier (Fig. 6). The CVL gas-discharge tubes were of the sealed type and specified for a maximum radiation power of 12 W. Owing to the use of a dye amplifier pumped by part of the radiation of the same CVL's, the radiation power of the dye laser used for the third excitation step could be increased several times. The spectral line width of the dye lasers was  $0.8 \text{ cm}^{-1}$ , and their average radiation power attained  $P = 1$  W.

The resonance ionization of Yb, Tm and Sn can be achieved in three steps as shown in Fig. 7. To excite the tin, it was necessary to use ultraviolet radiation in the first step. For saturation of the first and second transitions in the case of Yb and Tm it was sufficient to have a

laser output power of  $P \approx 300$  mW. The power of the second harmonic of the radiation of the dye laser used for exciting the first transition in tin was  $P \approx 3$  mW at the output of a non-linear crystal. Despite the losses occurring during transport into the ionizer, the first transition in tin was close to saturation. The final ionization of the atoms investigated was achieved by a radiation power of  $P \approx 1$  W, which saturated the transitions to autoionization states in Yb and Tm. In tin transitions to autoionizing states from excited intermediate states were not known prior to the start of our experiments [14]. Consequently ionization of tin was done via excitation into the continuum and saturation of the third transition was not achieved. This led to a substantially lower efficiency of the ion source for tin as compared to the case of Yb and Tm.

The three dye-laser beams were shaped by means of a mirror-lens optical system into a beam with an overall diameter of  $\approx 30$  mm, equal to the diameter of the aperture in the magnet, and with a diameter of the individual beams of  $\approx 15$  mm. The distance between the last lens of the optical system and the ionizer tube was in the case of ISOLDE-3 15 m. Under these circumstances the laser radiation divergence should be close to the diffraction limit, in order to focus the laser radiation into a spot of 1-mm diameter. This could not always be achieved, and the result was a reduction in laser radiation power in the capillary and a reduction in the photo-ion yield.

In the off-line experiments for which a large quantity of the element under examination was available, the radiation wavelength of the dye lasers was at first roughly determined with the aid of a monochromator and then precisely by the photo-ion signal. In the on-line experiments with radioactive isotopes, the radiation wavelength of these lasers was determined automatically with the aid of a micro-processor system with an accuracy of  $0.3 \text{ cm}^{-1}$ , which considerably simplified the process of tuning the laser radiation wavelength to the atomic resonances.

## **5. INFLUENCE OF THE IONIZER MATERIAL ON THE SELECTIVITY AND EFFICIENCY OF THE LASER ION-SOURCE**

The selectivity and efficiency of laser ionization and their dependence on the wall material were studied for Tm by means of the ISOLDE off-line mass separator. Different tubes were tried made of Ta, Nb or TaC to which Tm vapours were directed from an oven heated by a separate power supply (Fig. 8). The inside diameter of all the tubes used was 2 mm. The Ta and Nb tubes were 3 cm long, and the TaC tube was 2 cm long. In order to remove the mutual thermal influence, a cold, thick copper screen with an aperture of 2 mm was inserted between the tube and the oven. This design allowed to vary the temperature of the ionizer without changing the temperature of the Tm oven. In this way a controlled effusion of atoms into the capillary could be achieved. The photo-current at the output of the mass-separator was measured by means of a Faraday cup and did not exceed a few nA.

Figure 9 shows the dependences of the photo-current and surface-ionization current as function of the temperature of the tube and the material from which it was made. The surface-ionization current was measured without laser beams, whereas the photo-current was determined by subtracting the surface-ionization current from the total current. When changing from one tube material to another it was not possible to keep the Tm atom concentration constant in the capillary. However, since the radiation power of the lasers was strictly monitored and kept constant the probability of ionization by laser radiation was constant and did not vary when the tubes were changed. The data in Fig. 9 are therefore normalized to the maximum of the photo-current.

The behaviour of the curves shown in Fig. 9 can be explained as follows. When changing from Ta to Nb and TaC, the work function decreases from 4.12 eV to 3.65 eV, which results in an electron emission increase. The electron density at the surface of the TaC cavity is therefore higher than for the other materials. With an increase in the electron density, the absolute value of the plasma potential  $\Phi_p$  grows and the efficiency of photo-ion extraction increases. Consequently, in the low-temperature range, the value of the plasma potential created by TaC will still be adequate for retaining the photo-ions inside the plasma, while that created by Nb and Ta will not.

At decreasing temperature the surface ionization current drops faster than the photo-ion current due to a decrease in the plasma potential. The saturation of the photo-ion current at high temperature for Nb and particularly for TaC means that the potential well in which the photo-ions are retained is deep enough and almost all photoions are extracted.

Within the limits of accuracy of our experiment, a dependence of the surface-ionization current on the wall material could not be observed. This corresponds to the qualitative description of the processes in a hot cavity (eq. (8)), based on the assumption of attaining thermodynamic equilibrium inside it. It should, though, be remarked that the accuracy of the present experiment is not sufficient for unambiguous conclusions.

## 6. EFFICIENCY AND SELECTIVITY OF THE LASER ION-SOURCE

The efficiency of the laser ion-source was studied with radioactive isotopes of Yb in off-line and on-line operation. In the off-line experiments, an irradiated tantalum foil containing a known amount of radioactive Yb, determined by a Ge  $\gamma$ -spectrometer, was inserted into an empty tantalum target container. With the laser beam switched on, the target container with the foil and the ionizer were heated up to  $T \approx 2300$  K. The resulting ion beam of radioactive Yb was implanted into an aluminium foil. After total vaporization of the Yb out of the target container, the amount of Yb in the aluminium foil was determined by  $\gamma$ -spectrometry. The total efficiency of the laser ion-source was found to be  $10\% < \eta_{\text{capillary}} < 15\%$ . Similar experiments were performed with Tm activity induced in the foil. The measured efficiency was only 2%. A



search for the Tm activity showed that it was lost at the terminal ends of the target container which were too cold ( $T = 1900$  K) so that the major part of the activity was condensed here. By raising the temperature in this region it is expected that all the rare earth elements can be laser ionized with efficiencies of the order of 15%. In the on-line experiments carried out on ISOLDE-3 [15], the radioactive isotopes were produced by 600 MeV proton spallation of a thick tantalum target ( $122 \text{ g/cm}^2$ ). The ions were detected in the focal plane of the second magnet of ISOLDE-3 using a tape-transport system and the Ge(Li)  $\gamma$ -spectrometer. The efficiency and selectivity of the ion-laser source in the on-line operation were found to be similar to those obtained in the off-line experiments.

The selectivity  $S$  of the laser source is defined as the ratio of the photo-ion current to the surface ionization current. At low temperature ( $T = 1600$  K), the selectivity of the laser source reaches a value of  $S = 10^4$  for an ionizer made from TaC. At this temperature, the long sticking time of the atoms on the surface may cause losses of short-lived nuclei. With a rise in temperature the selectivity quickly falls and reaches  $S = 30$  at  $T = 2300$  K. Since the ionization efficiency of isobars is not affected by laser radiation, the ratio of the photo-ion signal of the isotope under investigation to the background signal of surface-ionized isobars is increased by this factor.

Ionization of tin was studied at the ISOLDE-3 mass-separator in off-line operating mode. Since tin has a high ionization potential ( $E_i = 7.3$  eV) the surface ionization efficiency of this element is considerably lower ( $\epsilon_{\text{surface}} \approx 0.006\%$ ) than that of rare-earth elements ( $\epsilon_{\text{surface}} \approx 1-10\%$ ). In the laser experiments the photoionization efficiency obtained was  $\eta_{\text{capillary}} = 0.2\%$ . It was determined by measuring the charge collected in a Faraday cup from a Sn-beam produced by evaporating a  $50 \mu\text{g}$  sample of Sn placed in the target. The selectivity of the ion-source was found to be  $S = 70$  for Sn. The low efficiency for Sn is explained by the fact that the ionization was performed by excitation into the continuum. The cross-section of this process is 1-2 orders of magnitude smaller than the cross-section for ionization via autoionizing states. Recently a new scheme of Sn ionization was found based on autoionizing states [14]. The cross-section of  $\sigma = 1.6 \cdot 10^{-16} \text{ cm}^2$  is high enough to attain saturation with the aid of the dye lasers used in our experiment. The efficiency and selectivity of the laser ion-source for Sn should now increase by two orders of magnitude to  $\eta_{\text{capillary}} \approx 10-20\%$  and  $S \approx 10^4$ , respectively.

Interesting information on the production of the element Li was obtained from a study of its laser ionization. An overall efficiency of  $\epsilon_{\text{surface}} = 5\%$  is obtained with surface ionizers combined with high-temperature Ta-targets at ISOLDE. Compared to the expected 90 % efficiency, this is in contrast to the other alkalis where the theoretical ionization efficiencies were readily obtained. When using the lasers for additional photo ionization of the nuclear reaction produced  ${}^7\text{Li}$  it was found that the laser ionization effect vanished when the surface ionizer reached its operating temperature. This indicates that a surface-ionization efficiency of indeed  $\epsilon_{\text{surface}} = 90\%$  was achieved. The fast diffusing Li seems therefore to be lost by

diffusion out through the wall of the Ta target container. Thus the 20 cm long and 122 g/cm<sup>2</sup> thick Ta target may be made considerable smaller without reducing the Li production.

## 7. TIME STRUCTURE OF THE PHOTO-ION CURRENT

Since the photo-ions are produced by pulsed lasers with a high pulse repetition rate, the obtained photo-ion beam is pulsed with the laser frequency. This pulsed structure of the beam allows the suppression of background from continuously surface ionized isobars by the aid of a beam gate which deflects the background ions during the pulse intervals.

The photo-ions are created during a short laser pulse of only about 20 ns duration. These ions are extracted from the capillary by a weak electric heating field  $E \approx 0.5$  V/cm. An ion with mass number  $A$  created at rest, inside the tube, at a distance  $s$  from the outlet of the source is extracted during the time

$$t_{\text{ex}} = 1.44 \sqrt{\frac{s \times A}{E}} \mu\text{s} \quad (10)$$

where the electric field  $E$  is given in V/cm and the distance  $s$  in cm. The time  $t_{\text{ex}}$  reaches a value of up to 50  $\mu\text{s}$  for an ion with mass number 174 created at the far end of a 3 cm long capillary, while an ion created at the outlet of the capillary is extracted immediately. Moreover the initial Maxwellian velocity distribution of the ions causes an additional spread of the time distribution. The time distribution is consequently determined by the initial density and velocity distribution of the photo-ions created in the capillary as well as by the extraction efficiency of the photo-ions. These properties are complex functions of the density and velocity distribution of the atoms irradiated by the laser light, the intensity distribution of the laser light, the temperature distribution and the plasma density in the capillary. For that reason an exact theoretical treatment of the problem is rather complicated.

After extraction from the capillary the ions are accelerated to a beam energy of  $E_a = 60$  keV and pass through the mass separator. The time  $t_{\text{flight}}$  to reach a point at distance  $l$  from the extraction electrode consists of the time of acceleration along a distance  $s_a = 0.06$  m and the time of flight through the mass separator over the distance  $l$ . This time is given by

$$t_{\text{flight}} = 2.28(l + 2s_a) \times \sqrt{\frac{A}{E_a}} \mu\text{s} \quad (11)$$

Here, the beam energy  $E_a$  is given in units of keV and the distances  $l$  and  $s_a$  in units of meters. The initial potential energy of the ions due to the electric field along the capillary and their thermal energy as well as the differences in the length of the path  $l$  through the mass separator

can be neglected, so that the time  $t_{\text{flight}}$  is essentially the same for all ions and does not effect the shape of the ion pulse.

To measure the pulse shape an electrostatic beam gate located between the two magnets of the ISOLDE-3 mass separator (Fig. 10) was used which allows the ions to pass during a short time window of about  $5 \mu\text{s}$  with variable delay relative to the laser pulse. The photo-ion current was measured behind the beam gate in a Faraday cup for different delays of the time window. In this way the pulse shape was measured for stable Yb for different currents along the capillary corresponding to different electric fields inside the capillary (Fig. 11). As expected, the pulse width was reduced with increasing electric field along the capillary. The measured pulse width of  $10 \mu\text{s}$  was much smaller than the  $t_{\text{ex}} = 50 \mu\text{s}$  expected for extraction of all ions from the tube. This pulse width is ten times smaller than the length of the intervals between the laser shots. This allowed an increase in the selectivity by one order of magnitude by closing the beam gate during the pauses. But surprisingly almost no ions were detected at  $t_{\text{flight}} = 62 \mu\text{s}$  which corresponds to ions created at the outlet of the capillary. The same striking result was also observed for Yb at the off-line separator.

In some experiments at ISOLDE-3, the capillary was slightly misaligned due to thermal expansion, so that the axis of the capillary was inclined by a small angle relative to the laser beam. Under these conditions the pulse shape was monitored by the signal of a particle multiplier on an oscilloscope. An additional small peak was observed at the time  $t_{\text{flight}} = 62 \mu\text{s}$  originating from ions created at the outlet of the capillary and possibly produced by laser desorption. In these measurements a pulse width was observed larger than the one obtained with a well-aligned capillary.

The pulse shape was also measured for  $^{120}\text{Sn}$  at ISOLDE-3 in off-line mode by the aid of the beam gate with variable delay (Fig. 12). In this case the onset of the ion pulse was observed at the expected time of  $t_{\text{flight}} = 51 \mu\text{s}$  and also the observed pulse width corresponds to the time  $t_{\text{ex}} = 50 \mu\text{s}$  required to extract all ions from the cavity. This relatively large pulse width allowed an increase the selectivity by a factor of 2 only in the case of tin. To achieve a shorter pulse and hence a larger selectivity, it is necessary to increase the electric extraction field in the capillary considerably. Because of the relatively low resistivity of metals an increase of the electric field of at least one order of magnitude is only possible using materials like graphite or ceramics with high resistivity.

## 8. CONCLUSION AND OUTLOOK

The test measurements performed under on-line conditions at the mass separator ISOLDE-3 showed the strength of the laser ion-source principle for efficient and selective ionization of short-lived isotopes. A chemical selectivity factor of 100 combined with efficiencies of the order of 10-20 % enables the study of a number of exotic, short-lived nuclei far from  $\beta$ -stability, where the use of conventional ion sources is hindered due to isobaric background. If

frequency doubling is applied in the first excitation step, also efficient photo-ionization of elements with ionization potentials as high as 7.3 - 7.6 eV like manganese, silver and tin (Fig. 13) can be achieved. For these elements very strong UV-transitions can be used in the first excitation step, which allows to reach saturation with the limited power available in the UV-wavelength range. By means of transitions to autoionizing states, saturation can be achieved in all excitation steps.

In the case of elements which do not react with oxides or nitrides, as for example silver, a shorter ion bunch and consequently an increased selectivity may be achieved by using a ceramic tube as laser ionizer, Fig. 5. This material allows to use an extraction voltage applied across the tube of up to 60 V, which is the energy spread acceptance of the separator.

An additional increase in selectivity may be achieved by an electrode system placed between the ionizer tube and the extraction electrode. The time focusing properties of such a system are well known from time-of-flight spectroscopy: An ion extracted from the target end of the ionizer tube is faster than the one extracted from the front end. Hence, the faster ion will reach the slower one after a certain drift length. An electrode configuration with an adequately varying potential can now be used to create a time focus of the extracted ions. A pulse width less than 1  $\mu$ s might be reached by this technique and may result in an enhancement of the selectivity by a factor of 100 or more.

An interesting candidate to be produced in high purity by the present laser ion-source technique is the extremely neutron-deficient, short-lived isotope  $^{102}\text{Sn}$  ( $T_{1/2} \approx 2$  s) near the doubly-magic  $^{100}/_{50}\text{Sn}_{50}$ . This isotope can be produced in the reaction  $^{50}\text{Cr} (^{58}\text{Ni}, 2p4n)$  using a 3 mg  $^{58}\text{Cr}$  target bombarded with a  $^{58}\text{Ni}$ -beam from the GSI-UNILAC at a beam current of 50 pA and an energy of 5 MeV/u. Simultaneously the isobars  $^{102}\text{In}$  and  $^{102}\text{Cd}$  are produced with much higher yields, so that a selective laser ion-source is required to ionize only the  $^{102}\text{Sn}$ .

At the new PS-BOOSTER-ISOLDE [16], an experiment is proposed for the investigation of the extremely neutron-rich, short-lived ( $T_{1/2} \approx 140$  ms) isotope  $^{129}\text{Ag}$ , one of the very few r-process "waiting-point" nuclei produced in terrestrial laboratories [17]. The  $\beta$ -decay half-life of this isotope is directly related to the observed r-abundance of the stable isobar  $^{129}\text{Xe}$  formed after  $\beta$ -decay of  $^{129}\text{Ag}$ . As can be inferred from the investigation of its isotone  $^{130}\text{Cd}$  [18], the measurement of  $^{129}\text{Ag}$  requires a selective ion source to suppress the isobaric background from  $^{129}\text{In}$  and the contaminating  $^{40}\text{Ca}^{89}\text{Br}^+$  molecule.

Selective ionization is also required in order to use the abundantly produced Mößbauer nuclide  $^{57}\text{Mn}$  for materials research. Due to impurities in the target and the presently used unselective ion sources an intense isobaric  $^{57}\text{Fe}$  beam destroys the substrates and may only be suppressed by means of selective laser ionization.

Finally, the laser source itself might be used for determination of nuclear ground state properties like spins, moments and charge radii via a determination of the hyperfine structure

splittings and isotope shifts. Generally, optical spectroscopy in the laser ion-source will be Doppler-limited and hence restricted to the investigation of heavy isotopes where the hyperfine splittings and isotope shifts are large. In special cases, Doppler-free techniques like two photon spectroscopy might be applied in order to study also light isotopes. An interesting application would be to study the isotopes of refractory elements for example Osmium which is not available as an on-line beam but are produced as daughter of the volatile Hg. The Hg atoms could be accumulated in the capillary of the ion source kept at low temperature while they decay to the daughter isotope under investigation. After heating the capillary, the daughter atoms are released and laser ionized. In such a scheme, The ISOLDE mass-separator would serve as a highly efficient and mass-selective detector device.

### **ACKNOWLEDGEMENTS**

This work was supported by the German Federal Minister for Research and Technology (BMFT) under contract number 06HZ 188-I.

## FIGURE CAPTIONS

- Fig. 1: Schematic representation of the mass-separator and laser ion-source.
- Fig. 2: Typical process of atom excitation and ionization by laser radiation.
- Fig. 3: Laser ionization of atoms a) in an atomic beam, b) in a hot cavity and c) in a hot cavity in the shape of a capillary.
- Fig. 4: Trajectory of photo-ion motion in a capillary where the heating potential applied to the ends of the capillary gives at the same time rise to an electric field along the tube axis which ejects the ions.
- Fig. 5: Schematic representation of the target and ionizer used in the experiments at the ISOLDE-3 mass separator.
- Fig. 6: Laser system used for resonance laser ionization of atoms. M: mirror, L: lens, D: dye-cell amplifier.
- Fig. 7: Atomic transitions used for laser ionization of Yb, Tm and Sn.
- Fig. 8: Oven and ionizer assembly used for studies of the influence of the wall material on the selectivity and efficiency of the laser ion-source.
- Fig. 9: Dependence of the photo-ion current and the surface ionization current of Tm on the temperature of the ionizer tube and on the material the tube is made of.
- Fig. 10: Laser ion-source at the on-line separator ISOLDE-3. The ion optics (lenses and magnets) are shown for the horizontal plane. M: mirror, LB: laser beams, M1: first magnet, F1: focal point of the first magnet, M2: second magnet, PD: pulsed deflector, F2: focal point of the second magnet, ID: ion detector. Insert: Schematics of the target container, transfer tube, ionizer tube and extraction electrode of the laser ion-source.
- Fig. 11: Shape of photo-ion pulse observed at the exit of the second magnet of the ISOLDE-3 mass separator for stable  $^{174}\text{Yb}$ . The ionizer, a tantalum tube (length  $L = 3$  cm, inside diameter  $d = 1$  mm), was heated by a d.c. current of  $I = 95$  A (open squares) and  $I = 137$  A (asterisks). The solid curve is a fit of the experimental points by a Gaussian.
- Fig. 12: Pulse shape of the photo-ion current of stable Sn as obtained at the on-line mass separator ISOLDE-3. The ionizer, a tantalum tube (length  $L = 3$  cm, inner diameter  $d = 1$  mm) was heated by a dc current. The dashed line indicates the time of flight through the mass separator from the outlet of the ionizer. The solid lines indicate the laser pulses.
- Fig. 13: Atomic level schemes for resonance ionization of the elements silver, manganese and tin which have ionization potentials between 7.37 eV and 7.58 eV. A strong UV-transition is used in the first excitation step and a resonant transition to an autoionizing state in the third step.

## 9. REFERENCES

- [1] T. Bjørnstad, E. Hagebø, P. Hoff, E. Kugler, H.L. Ravn, S. Sundell, and B. Vosicki, *Phys. Scr.* 34 (1986) 578.
- [2] V.S. Letokhov, *Laser Photoionization Spectroscopy* (Academic Press, London, 1987).
- [3] V.N. Fedoseyev, V.S. Letokhov, V.I. Mishin, G.D. Alkhazov, A.E. Barzakh, V.P. Denisov, A.G. Deryatin and V.S. Ivanov, *Opt. Commun.* 52 (1984) 24.
- [4] Th. Hilberath, St. Becker, G. Bollen, H.-J. Kluge, U. Krönert, G. Passler, J. Rikowska and R. Wyss, *Z. Phys.* A342(1992)1.
- [5] S.V. Andreev, V.I. Mishin and S. K. Sekatskii, *Sov. J. Quantum Electron.* 15(1985)398.
- [6] H.-J. Kluge, F. Ames, W. Ruster and K. Wallmeroth, *Proc. of the Accelerated Radioactive Beams Workshop, Parksville, Canada, 1985*, ed. L. Buchmann, J.M. D'Auria, TRIUMF, Canada, TRI-85-1, p. 119.
- [7] F. Scheerer, V.N. Fedoseyev, H.-J. Kluge, V.S. Letokhov, V.I. Mishin, H.L. Ravn, Y. Shirakabe S. Sundell, and O. Tengblad, *Proc. 4th Int. Conf on Ion Sources*, 30. Sept.-4. Oct. 1991, Bensheim Germany, *Rev. Sci. Instrum.*, 63 (1992) 2831.
- [8] F. Ames, T. Brumm, K. Jäger, H.-J. Kluge, B. Suri, H. Rimke, N. Trautmann and R. Kirchner, *Appl. Phys.* B51 (1990) 200.
- [9] S.V. Andreev, V.I. Mishin and V.S. Letokhov, *Opt. Commun.* 57 (1986) 317.
- [10] S.V. Andreev, V.I. Mishin and V.S. Letokhov, *J. Opt. Soc. Am.* B5 (1988) 2190.
- [11] G.D. Alkhazov, E.Ye. Berlovich and V. N. Panteleev, *Nucl. Instrum. & Methods* A280 (1989) 141.
- [12] R. Kirchner, *Nucl. Instrum. & Methods* 186 (1981) 275.
- [13] M. Huyse, *Nucl. Instrum. & Methods* 215 (1983) 1.
- [14] F. Scheerer, F. Albus, F. Ames, H.-J. Kluge, and N. Trautmann, *Spectrochimica Acta*, 47B (1992) 793.
- [15] B.W. Allardyce and H.L. Ravn, *Nucl. Instrum. & Methods* B26 (1987) 112.
- [16] E. Kugler, D. Fiander, B. Jonson, H. Haas, A. Prezewloka, H.L. Ravn, D.J. Simon, K. Zimmer and the ISOLDE Collaboration, *Nucl. Instrum. Methods* B70 (1992) 41.
- [17] K.-L. Kratz, *Rev. Mod. Astronomy* 1 (1988) 184.
- [18] F. Käppeler, H. Beer and K. Wisshek, *Rep. Prog. Phys.* 52 (1989) 345.

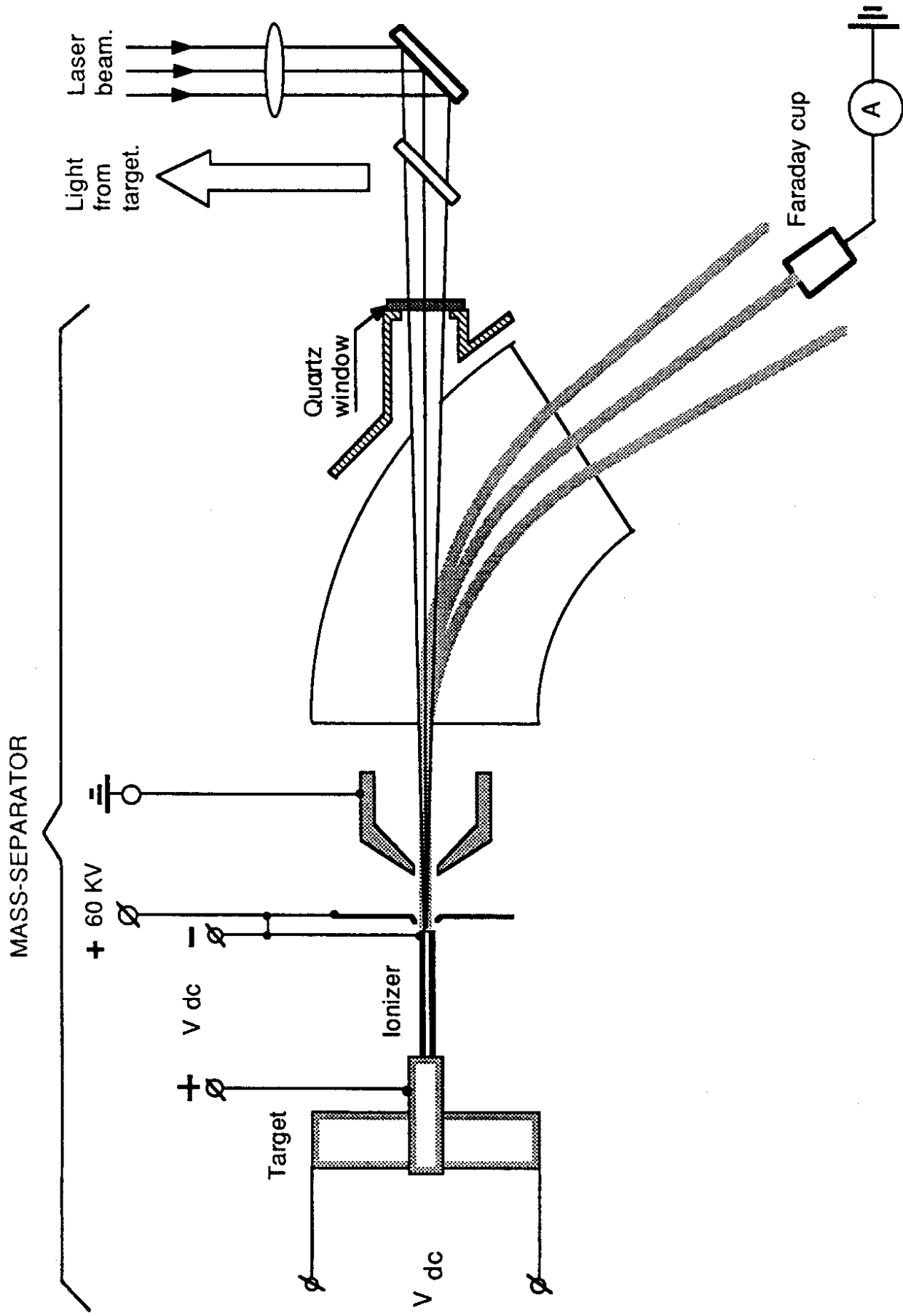


Fig. 1



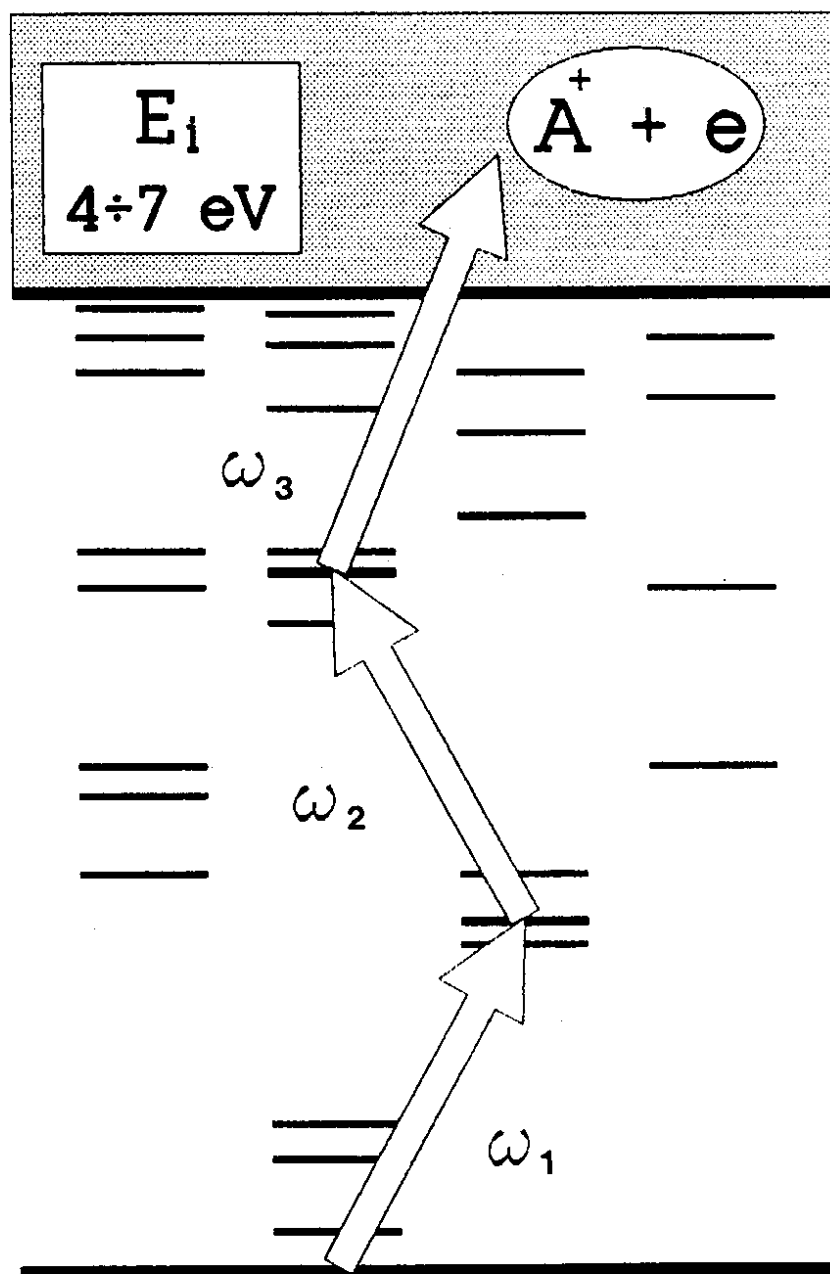


Fig. 2

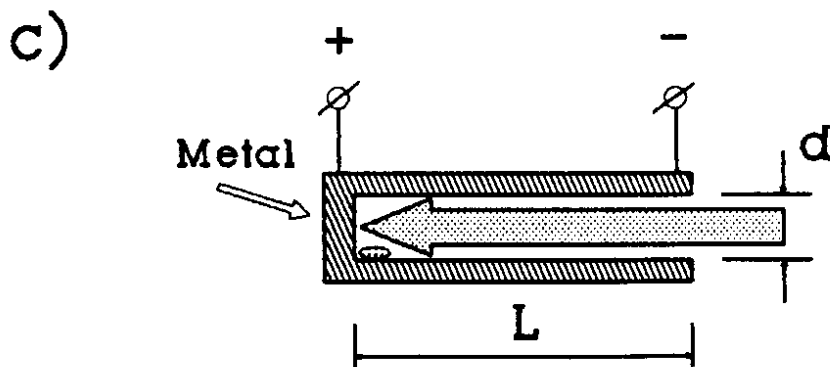
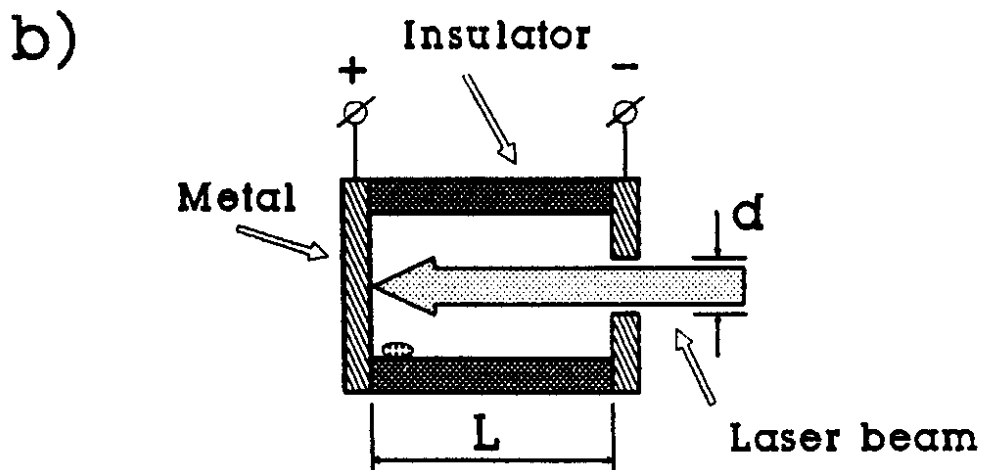
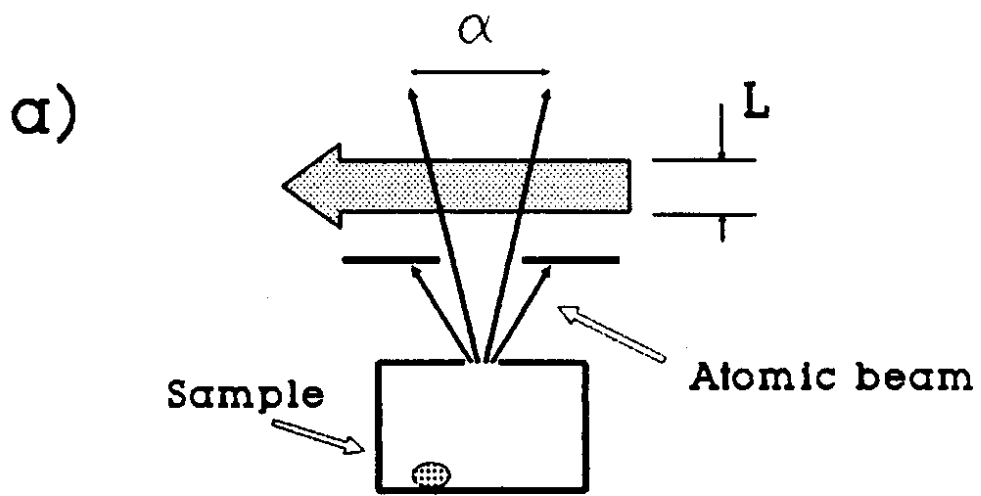


Fig. 3

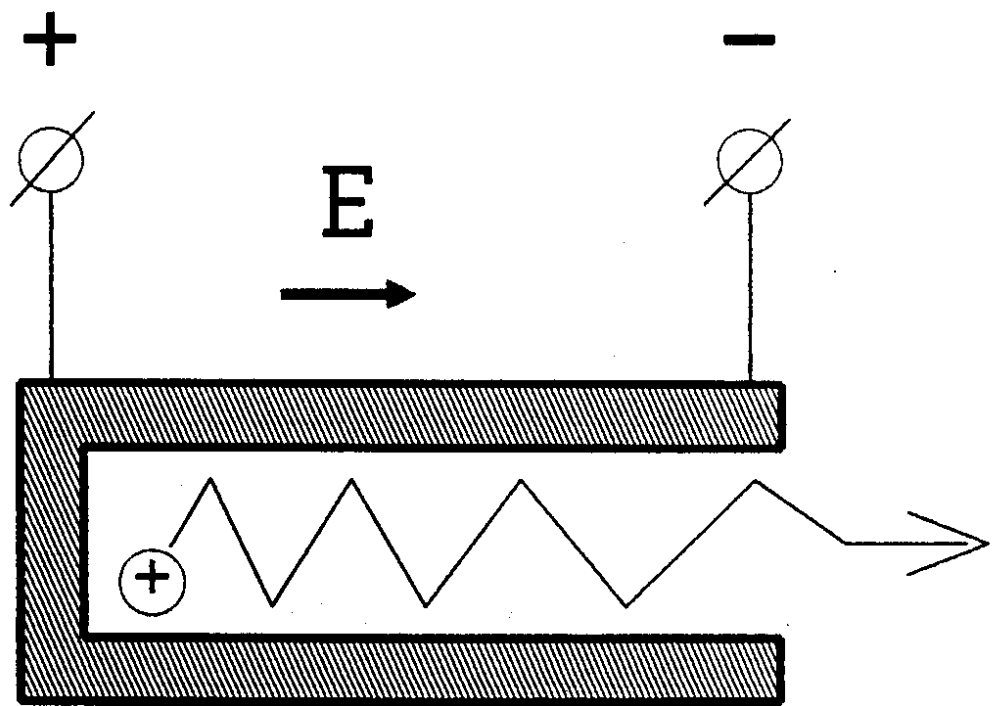


Fig. 4

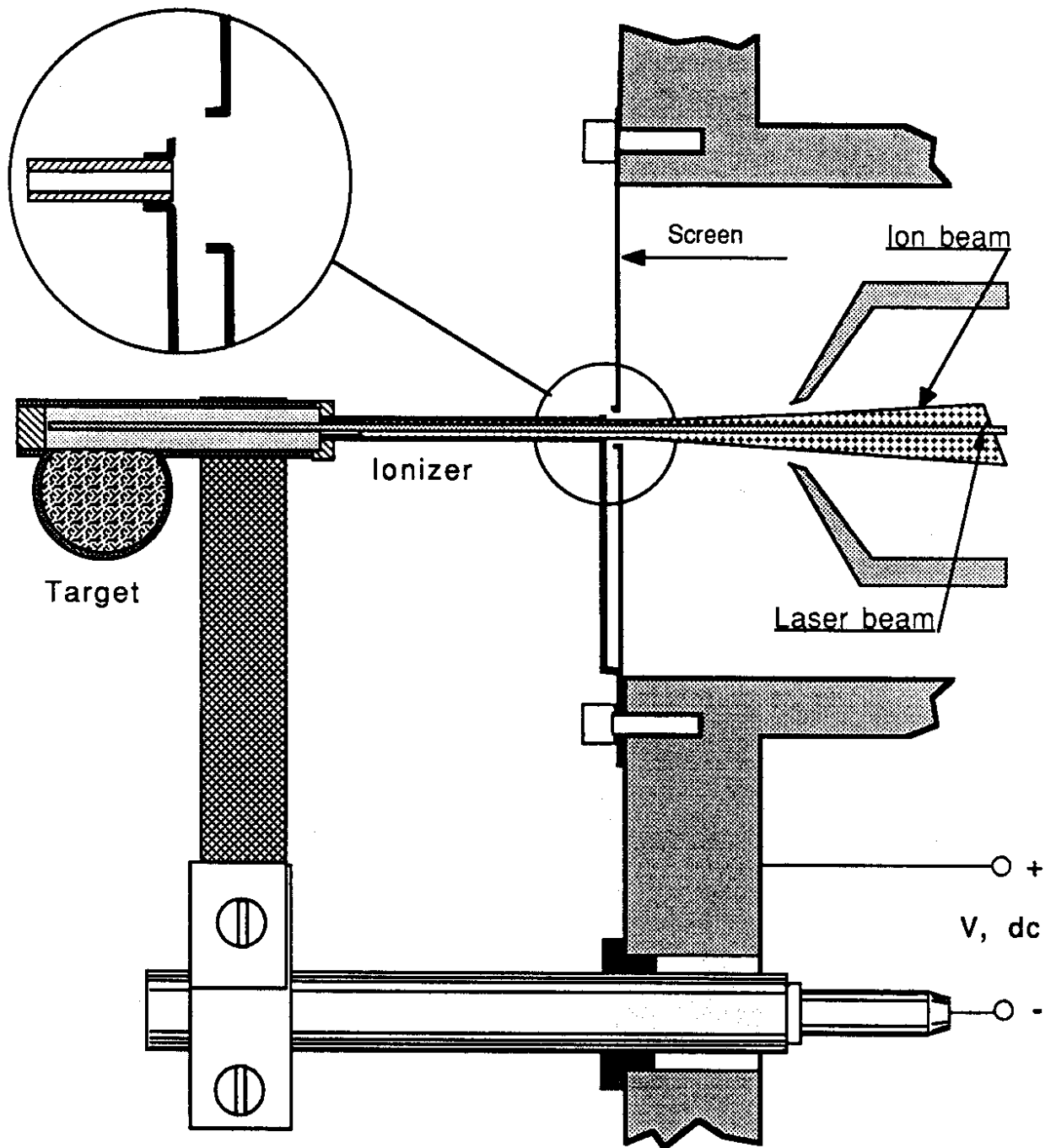


Fig. 5

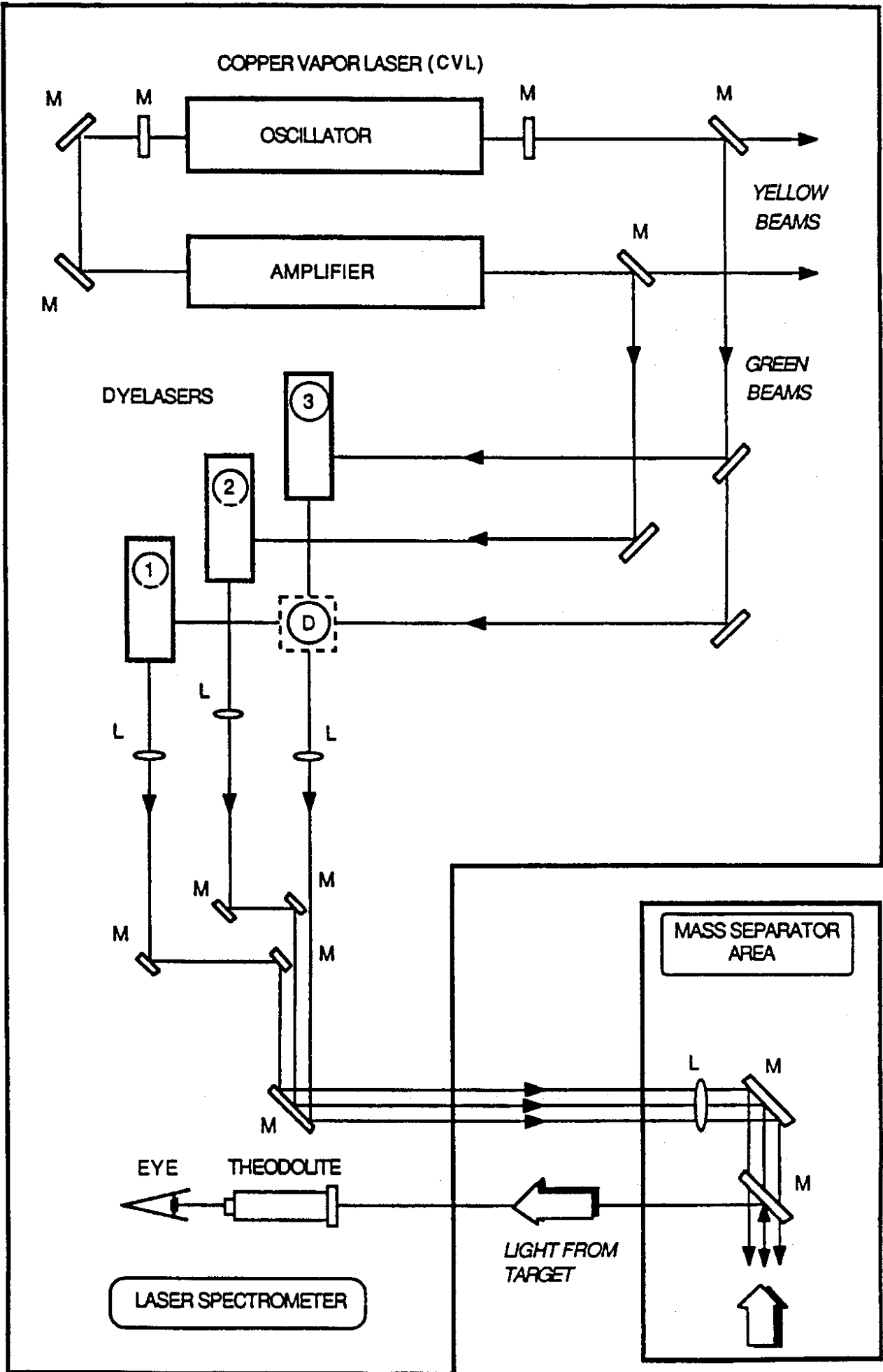


Fig. 6

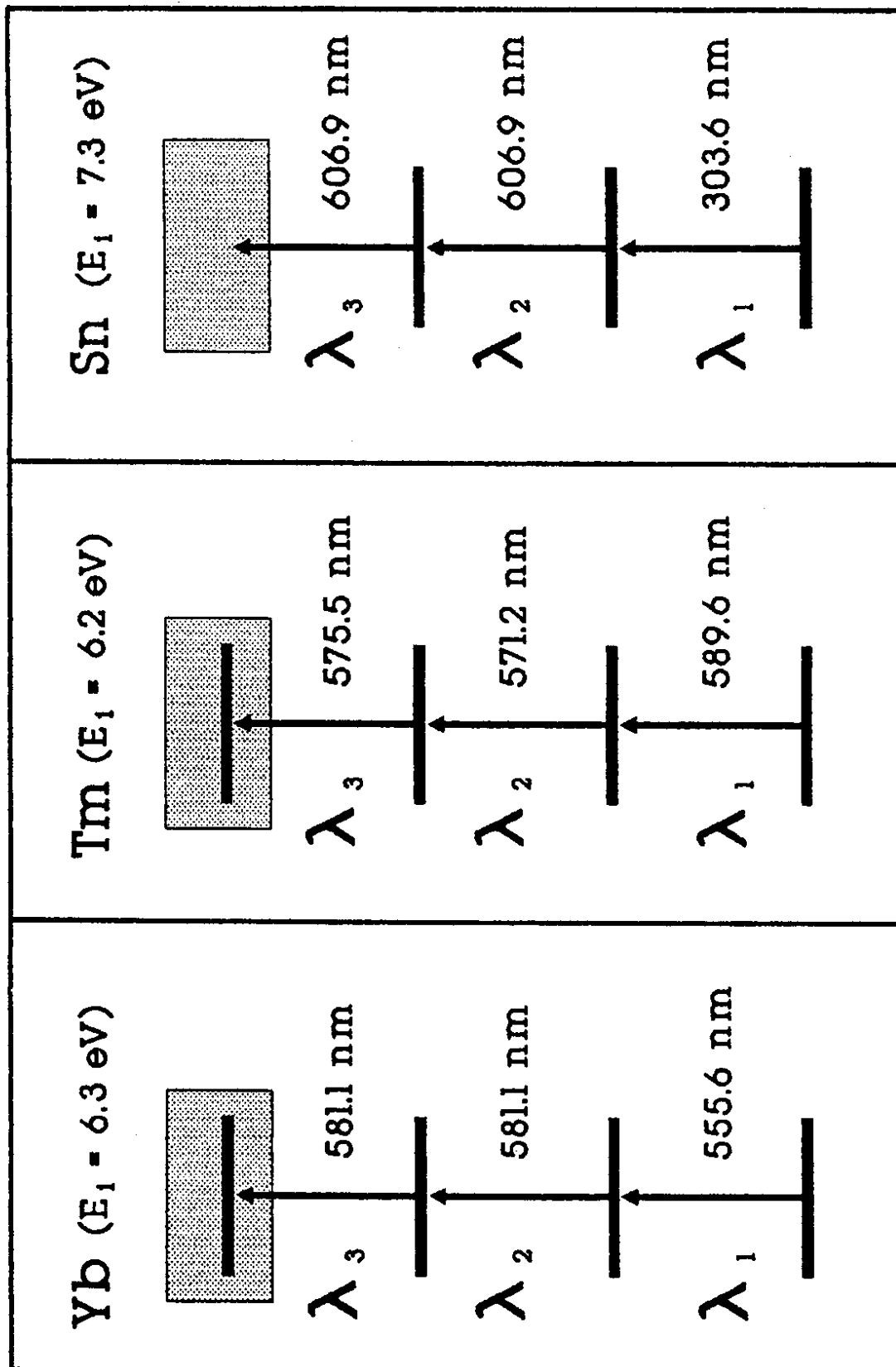


Fig. 7

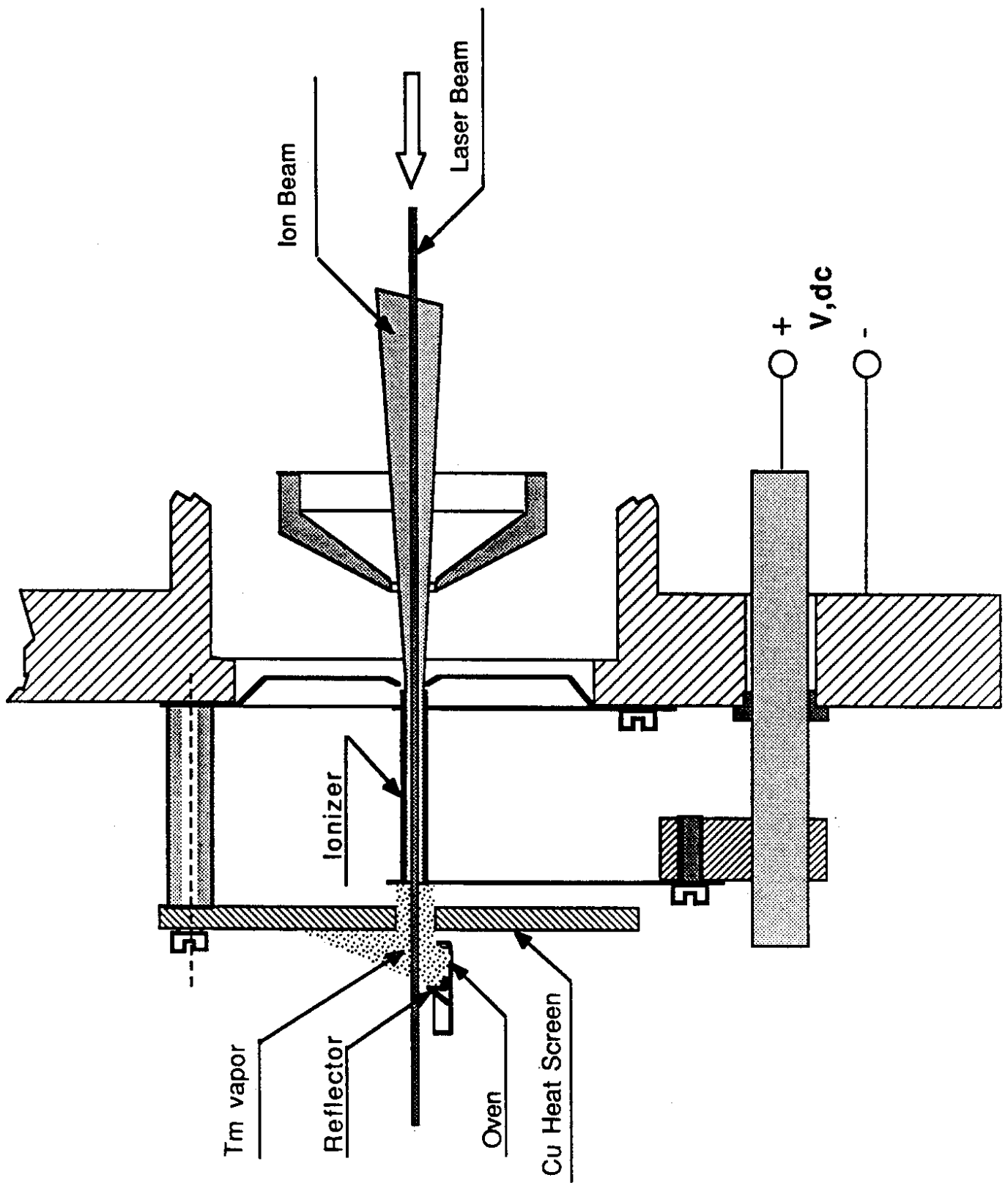


Fig. 8

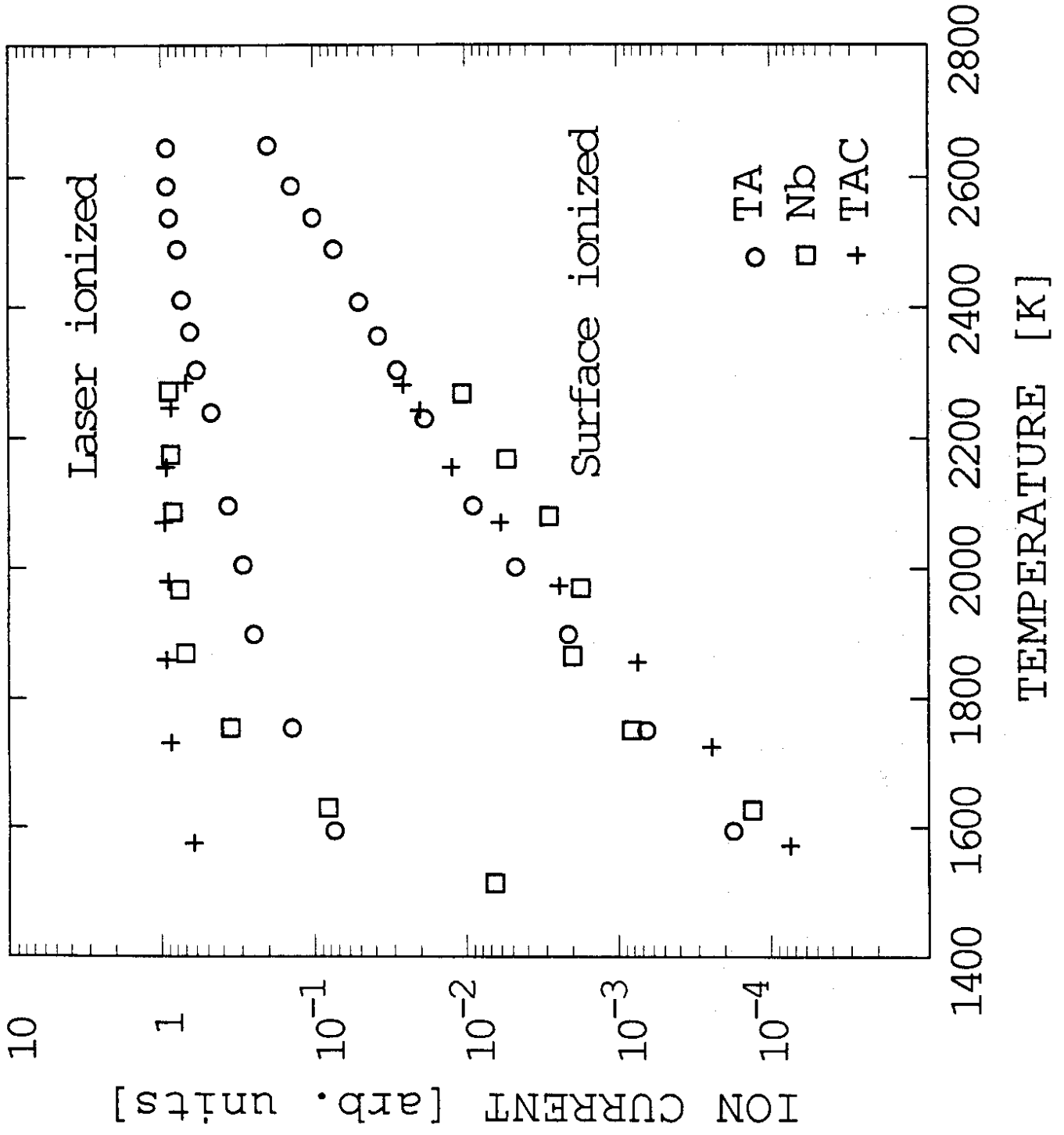
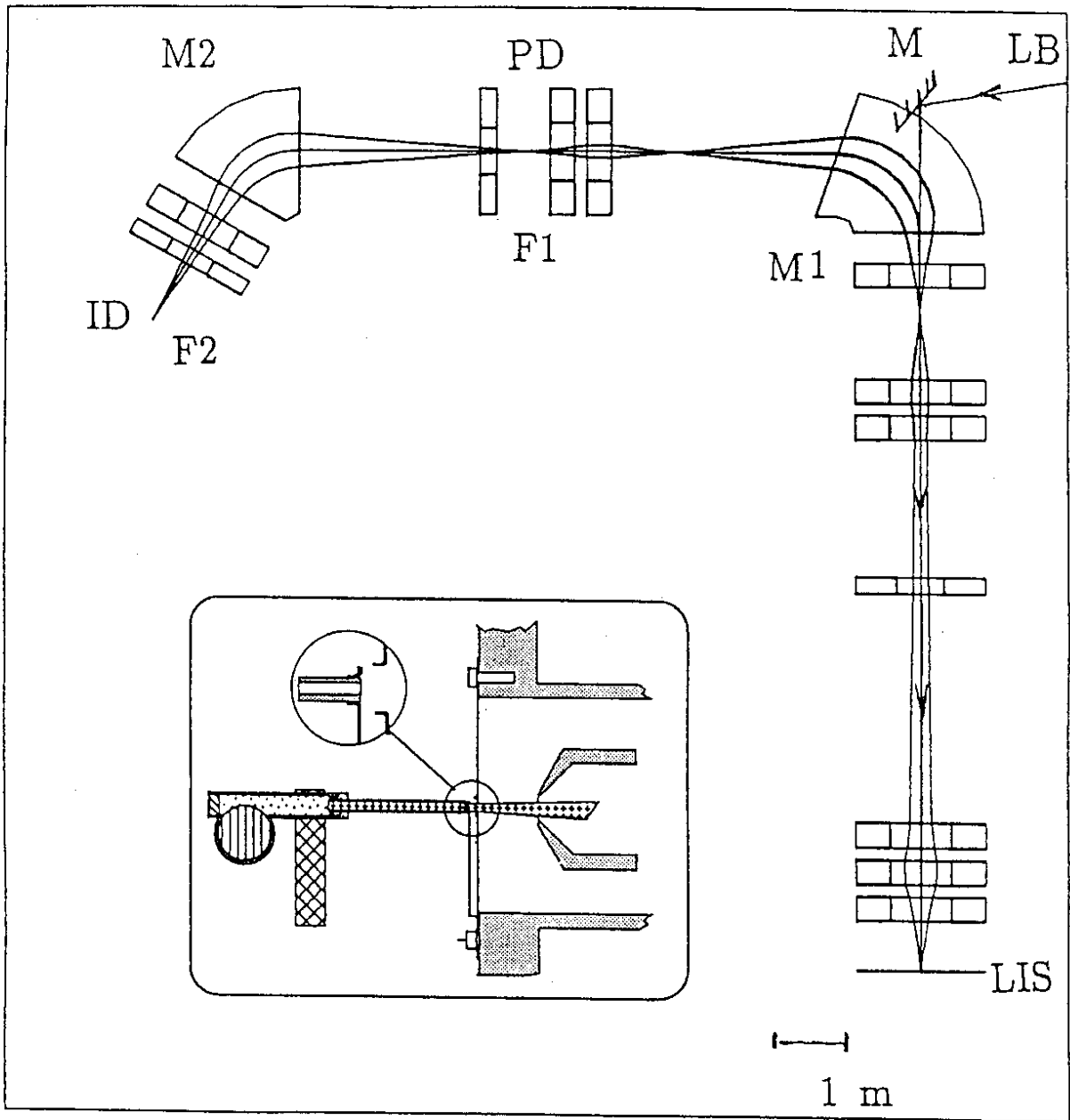


Fig. 9





Inst. f. Phys., Mz. 91676

Fig. 10

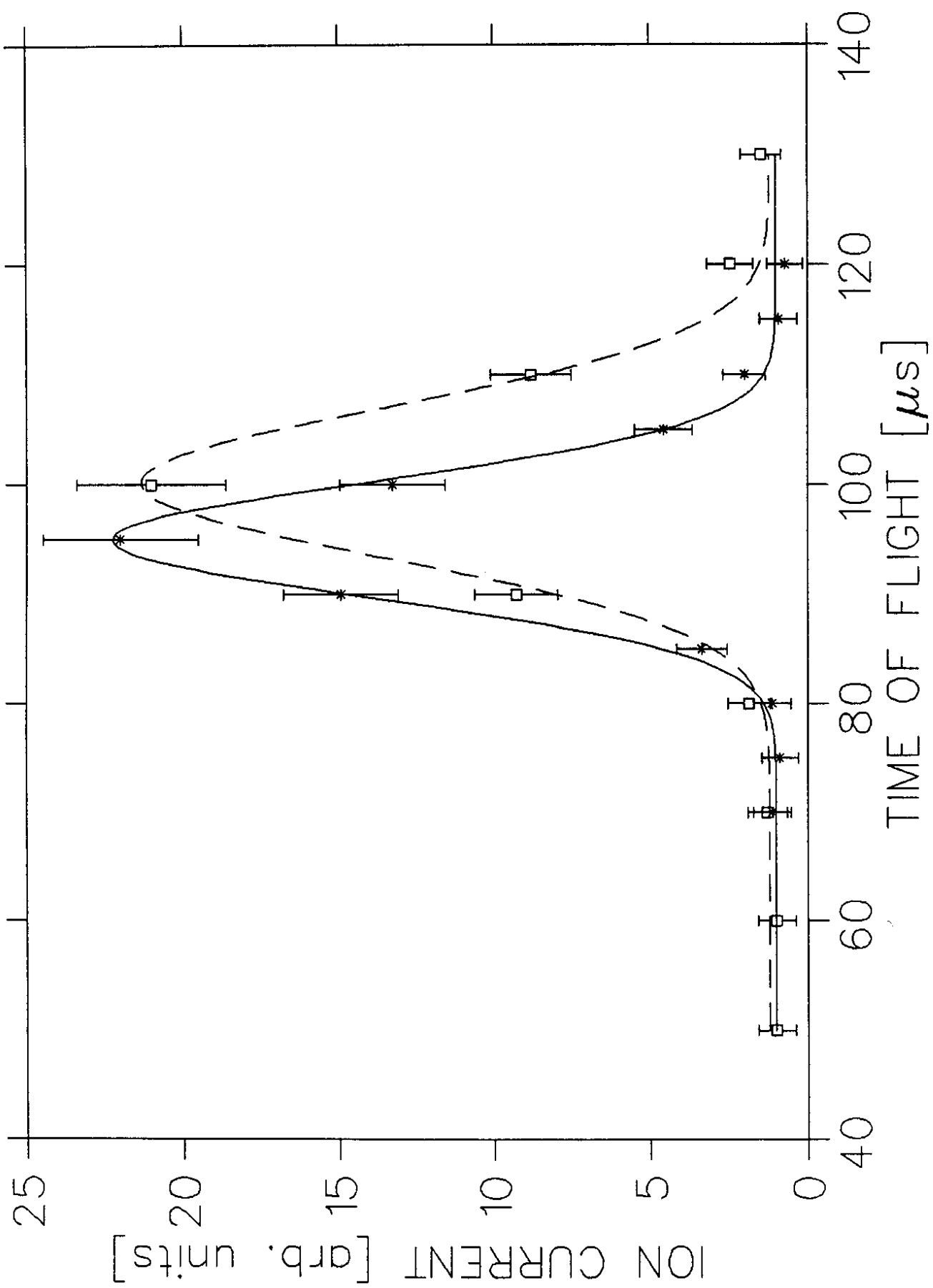


Fig. 11

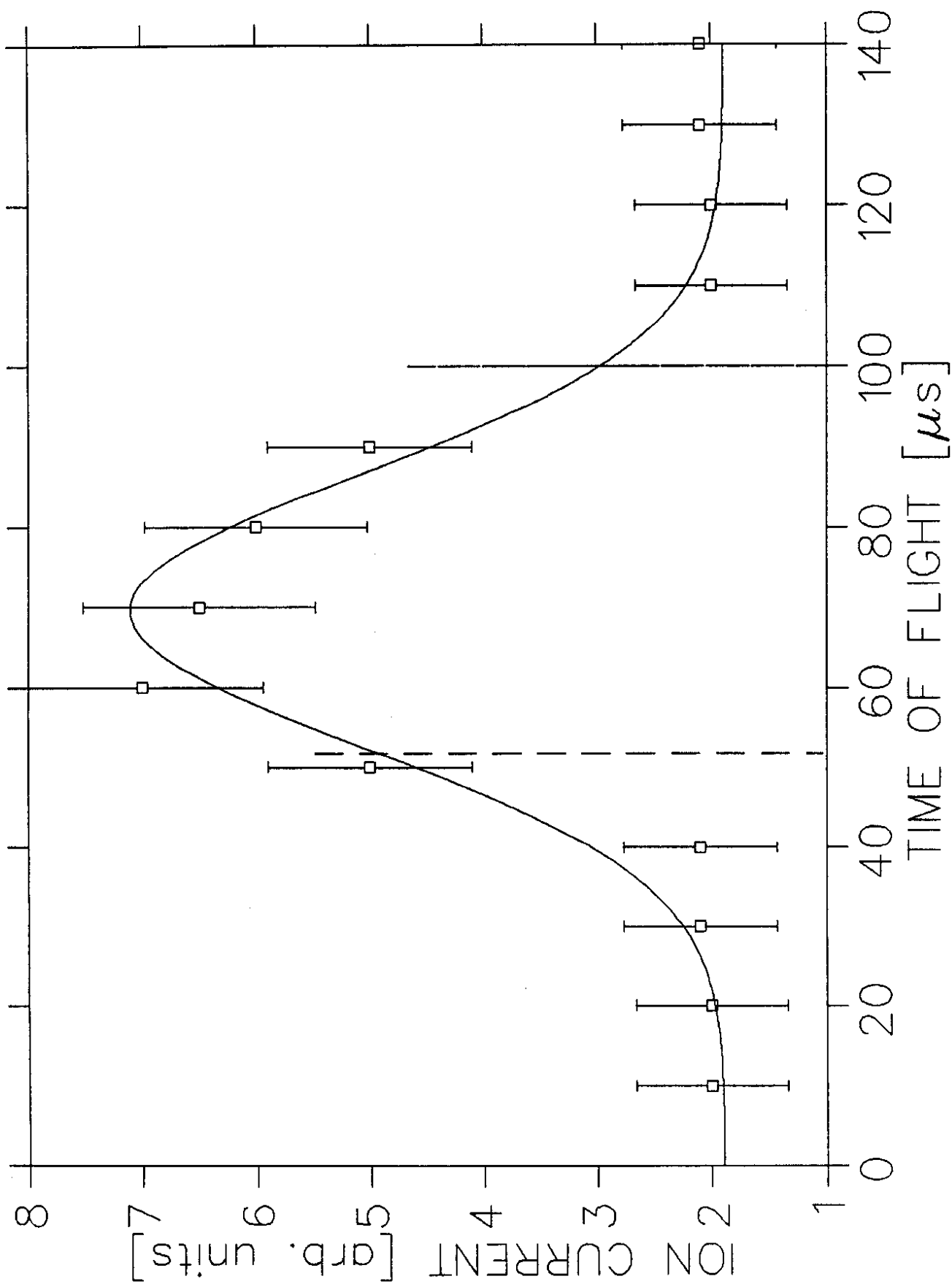


Fig. 12

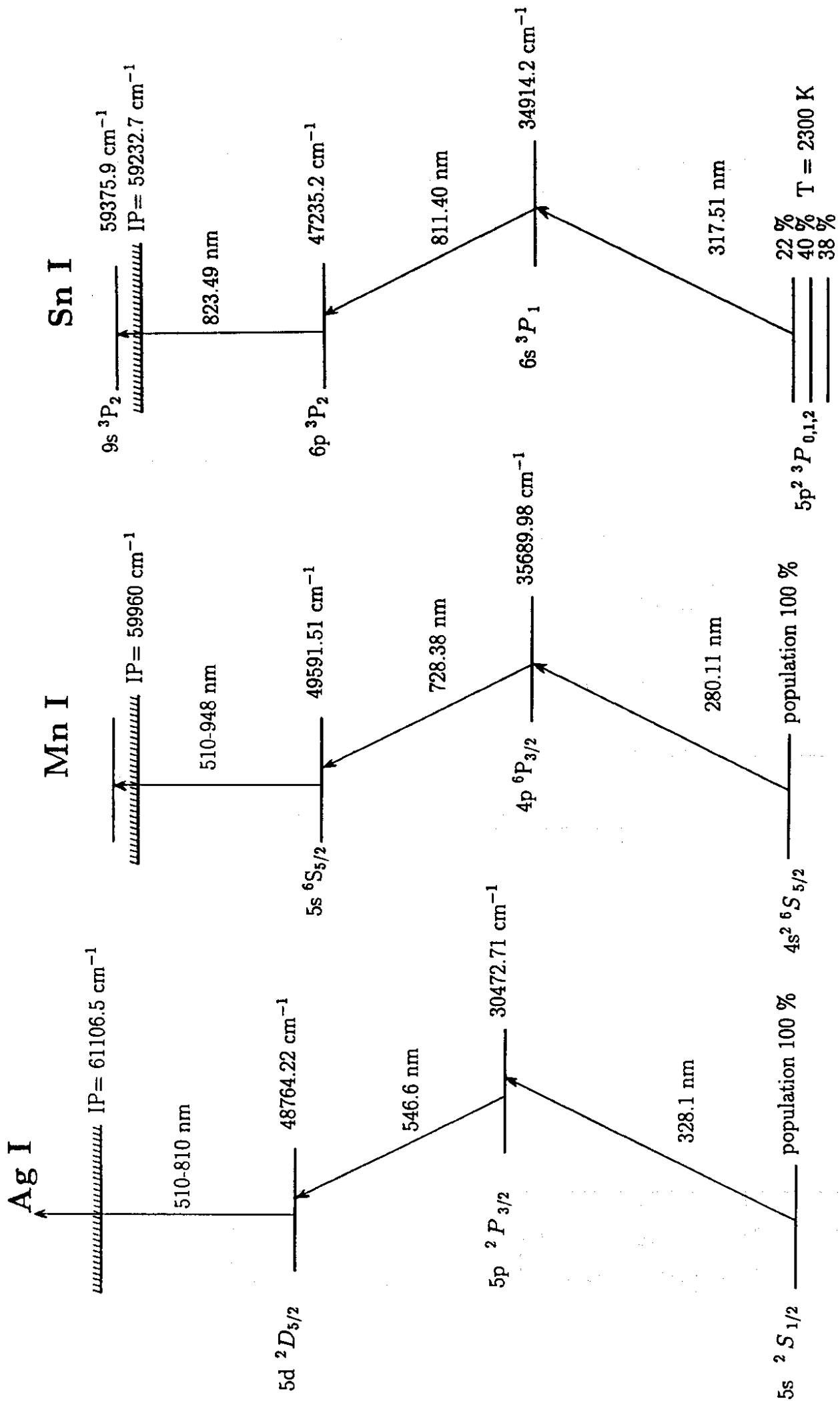


Fig. 13